

A regolith lead isoscape of Australia

Candan U. Desem¹, Patrice de Caritat², Jon Woodhead¹, Roland Maas¹, Graham Carr³

¹School of Geography, Earth and Atmospheric Sciences, The University of Melbourne, Melbourne, VIC 3010, Australia

²Geoscience Australia, GPO Box 378, Canberra, ACT 2601, Australia

³Commonwealth Scientific and Industrial Research Organisation, North Ryde, NSW, Australia

Correspondence to: Candan Desem (candandeseem@gmail.com)

Abstract. We present the first national-scale lead (Pb) isotope maps of Australia based on surface regolith for five isotope ratios, $^{206}\text{Pb}/^{204}\text{Pb}$, $^{207}\text{Pb}/^{204}\text{Pb}$, $^{208}\text{Pb}/^{204}\text{Pb}$, $^{207}\text{Pb}/^{206}\text{Pb}$, and $^{208}\text{Pb}/^{206}\text{Pb}$, determined by single collector Sector Field-Inductively Coupled Plasma-Mass Spectrometry after an Ammonium Acetate leach followed by Aqua Regia digestion. The dataset is underpinned principally by the National Geochemical Survey of Australia (NGSA) archived floodplain sediment samples. We analysed 1219 samples (0-10 cm depth, <2 mm grain size), collected near the outlet of 1119 large catchments covering 5.647 million km² (~75% of Australia). The samples consist of mixtures of the dominant soils and rocks weathering in their respective catchments (and possibly those upstream) and are therefore assumed to form a reasonable representation of the average isotopic signature of those catchments. This assumption was tested in one of the NGSA catchments, within which 12 similar samples were also taken; results show that the Pb isotope ratios of the NGSA catchment outlet sediment sample are close to the average of the 12 sub-catchment, upstream samples. National minimum, median and maximum values reported for $^{206}\text{Pb}/^{204}\text{Pb}$ were 15.56, 18.84, 30.64; for $^{207}\text{Pb}/^{204}\text{Pb}$ 14.36, 15.69, 18.01; for $^{208}\text{Pb}/^{204}\text{Pb}$ 33.56, 38.99, 48.87; for $^{207}\text{Pb}/^{206}\text{Pb}$ 0.5880, 0.8318, 0.9847; and for $^{208}\text{Pb}/^{206}\text{Pb}$ 1.4149, 2.0665, 2.3002, respectively. The new dataset was compared with published bedrock and ore Pb isotope data, and was found to dependably represent crustal elements of various ages from Archean to Phanerozoic. This suggests that floodplain sediment samples are a suitable proxy for basement and basin geology at this scale, despite various degrees of transport, mixing, and weathering experienced in the regolith environment, locally over protracted periods of time. An example of atmospheric Pb contamination around Port Pirie, South Australia, where a Pb smelter has operated since the 1890s, is shown to illustrate potential environmental applications of this new dataset. Other applications may include elucidating details of Australian crustal evolution and mineralisation-related investigations. The new regolith Pb isotope dataset for Australia is publicly available (Desem et al., 2023; <http://dx.doi.org/10.26186/5ea8f6fd3de64>).

1 Introduction

Isoscapes – isotopic maps of landscapes – are increasingly used as tools to address a wide range of research questions in fields as diverse as hydrochemistry (e.g., Bowen et al., 2009), forensic studies (e.g., Chesson et al., 2014), and tracking animal migrations (e.g., Hobson et al., 2010). Isotopic maps of the element strontium (Sr) in particular, often constructed at large

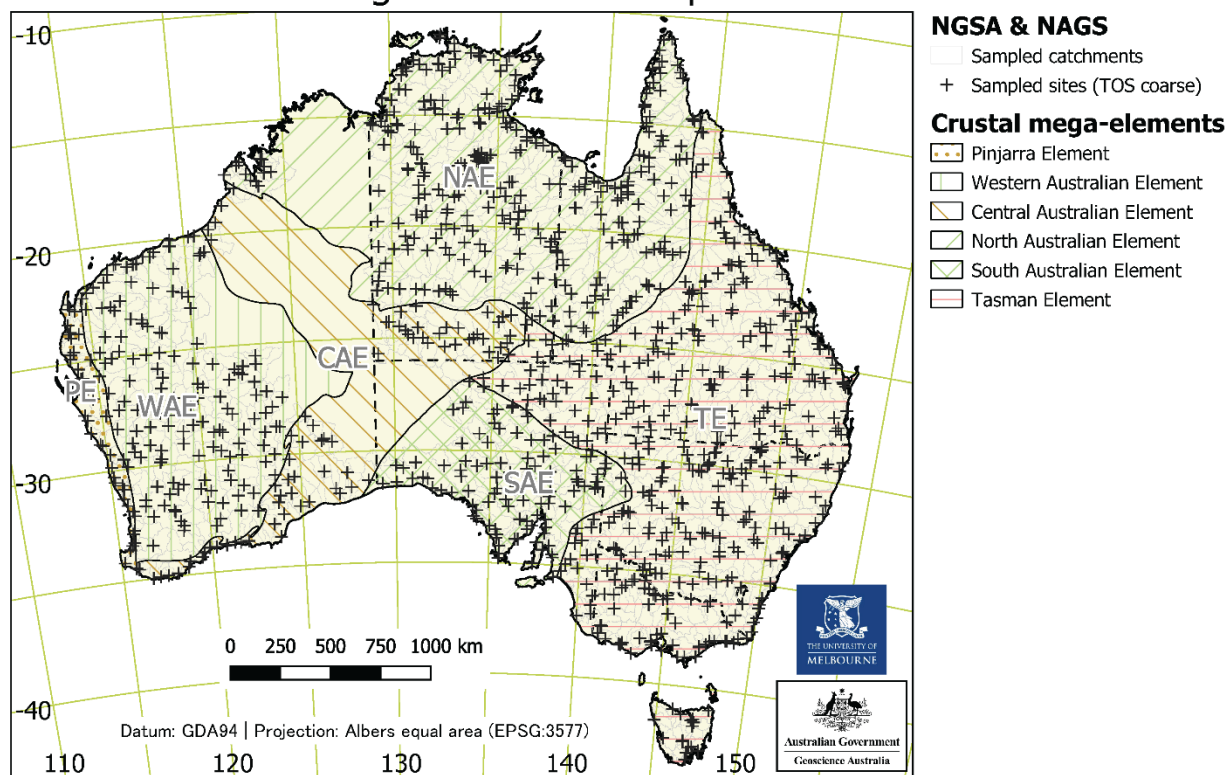
31 scale, are finding increasing utility in provenance studies (e.g., Adams et al., 2019; Willmes et al., 2018; Bataille et al., 2020;
32 Scaffidi and Knudson, 2020; de Caritat et al., 2022, 2023). The utility of Sr in this regard stems from its high bioavailability,
33 coupled with its relative ease of isotopic determination in soil, water, and animal and plant tissue.

34 One limitation of Sr as a tracer is that it has only one radiogenic isotope ratio ($^{87}\text{Sr}/^{86}\text{Sr}$), hence a single isotopic determination
35 on a target material may match multiple natural occurrences of that value across an isoscape. In contrast, the element lead (Pb)
36 offers greater resolving potential; its isotopic composition is the result of three independent radioactive decay chains, producing
37 effectively ‘three tracers in one’ and, as a result, much greater potential for accurate source attribution. Pb isotopes have, in
38 fact, been used for many decades in provenance determination where metallic archaeological objects such as coins, shipwreck
39 anchors, lead ingots, etc., have been traced to the likely sources from which their ores were mined (e.g., Gale and Stos-Gale,
40 2000). A similar methodology has been applied to track the origin of basaltic stone tools (e.g., Weisler and Woodhead, 1995).
41 Pb is also a relatively bioavailable element, with well-known adverse effects on human health due to its cumulative toxicity
42 and widespread use, and Pb isotopes have been used extensively to track the sources of Pb in humans (e.g., Gulson, 2008).

43 These existing Pb-isotope studies, however, typically rely on matching samples to known point sources and, as such, do not
44 employ the full predictive power of isoscapes, for example, allowing the estimation of likely values for regions that do not
45 have high sampling density. While Sr isoscapes are now in widespread use, the major impediment to the construction of
46 continental-scale Pb-isotope maps is primarily an analytical one: Pb-isotope analysis traditionally requires exacting clean-
47 room chemistry and specialised mass spectrometry procedures, and is correspondingly more expensive and time consuming
48 than Sr-isotope analysis. As a result, very few large-scale, empirical Pb-isotope isoscapes have been constructed – an
49 agricultural soil map of Europe (Reimann et al., 2012) and a tooth enamel study in Britain (Evans et al., 2022) being major
50 exceptions, with ongoing but smaller-scale studies in various other countries aimed at tracking anthropogenic contaminants
51 (e.g., Bing-Quan et al., 2002; Zuluaga et al., 2017), provenancing cultural materials (e.g., Hsu and Sabatini, 2019) and isotopic
52 changes in blood and teeth associated with migration between countries (Gulson et al., 1997; 2003, 2008)..

53
54 In this study, we release the first regolith Pb isoscapes constructed on a large scale for the Australian continent. Based upon
55 surface regolith samples collected during the National Geochemical Survey of Australia (NGSA; www.ga.gov.au/ngsa; de
56 Caritat and Cooper, 2011, 2016; de Caritat, 2022), these isoscapes are underpinned by a relatively dense and homogeneous
57 distribution of sampling sites across the continent (Figure 1). This work was made possible by technological developments
58 allowing both rapid and precise Pb-isotope analysis of large sample suites using an analytical method recently described in
59 Desem et al. (2022) and summarised below. The major advantage of this protocol over traditional methodologies for Pb-isotope
60 analysis is it does not require matrix separation, thus greatly streamlining the analysis of large sample suites.

Regolith Lead Isoscape of Australia



61
62 **Figure 1. Map showing the location of the National Geochemical Survey of Australia (NGSA) and Northern Australia Geochemical**
63 **Survey (NAGS) sampling sites (black crosses) and NGSA catchments (grey polygons) (de Caritat and Cooper, 2011; Main et al.,**
64 **2019) overlain by crustal mega-elements (hatched polygons) (Shaw et al., 1998). The mega-elements are labelled as (west to east) PE:**
65 **Pinjarra Element; WAE: Western Australian Element; CAE: Central Australian Element; NAE: North Australian Element; and**
66 **TE: Tasman Element.**

67 **2 Materials and methods**

68 **2.1 Materials**

69 Our study principally utilises ‘catchment outlet sediment’ samples originally collected from two depths (top outlet sediment,
70 or TOS, from 0 to 10 cm depth, and bottom outlet sediment, or BOS, from, on average, 60 to 80 cm depth) during the NGSA
71 project (de Caritat and Cooper, 2011, 2016; de Caritat, 2022), which covered ~80% of the Australian continent (for details on
72 sample collection, see Lech et al., 2007). At Geoscience Australia, freshly collected samples were air dried at 40 °C for a
73 minimum of 48 hrs (or to constant mass), homogenised, and reduced by riffle splitting, with half of each sample set aside in
74 an archive for future investigations, and the other half prepared for various analyses (for details on sample preparation, see de

75 Caritat et al., 2009). A ‘bulk’ split was retained for mineralogical analyses, another was sieved to a ‘coarse’ (<2 mm) grain-
76 size fraction, and yet another was sieved to a ‘fine’ (<75 µm) grain-size fraction. The latter two fractions of both depths were
77 then further prepared for the comprehensive geochemical analysis program of the NGSA (for details on sample analysis, see
78 de Caritat et al., 2010). Here, 1204 NGSA TOS coarse samples from 1098 catchments were used, with three of them analysed
79 twice for a total of 1207 analyses. Twelve additional TOS coarse samples collected in a similar manner to the NGSA samples
80 (from 0 to 10 cm depth and sieved to <2 mm) during the Northern Australia Geochemical Survey, or NAGS (Main et al.,
81 2019), were included in this study, giving a total of 1219 TOS coarse analyses underpinning the present isoscapes. In addition
82 to the above, 16 NGSA TOS fine (<75 µm) and 16 NGSA BOS coarse (<2 mm) were also analysed; although these data are
83 released herewith for the sake of completeness, they are not discussed further.

84 **2.2 Methods**

85 For the purpose of the Pb-isotope analyses, conducted at the University of Melbourne, the TOS coarse fractions from the
86 NGSA project were utilised. All samples to be analysed were subjected to a two-step sequential leaching protocol designed to
87 minimise and isolate any anthropogenic overprints on the primary Pb-isotope data. In the first step, an ammonium acetate
88 (AmAc) leach, developed at CSIRO and described in Carr et al. (2011), was applied to extract and remove any labile or loosely
89 bound/adsorbed components. Splits of ~1.2 g of sample were mixed with 6 mL of a 1:1 mixture of ultrapure water and
90 ammonium acetate buffer solution (AmAc; pH ~5). The soil/leach solution mix was shaken and left to react at 20 °C for 15
91 hours. Following centrifuging (4.5 min at 3000 rpm), a clear supernatant solution – the ‘AmAc leach’ or ‘A’ sample – was
92 pipetted off and dried in a high-efficiency particulate air (HEPA)-filtered fume-hood. In the second step, the remaining
93 undigested sample was subjected to an aqua regia (AR, 3:1 HCl:HNO₃) acid attack to digest most (though not all) of the more
94 refractory components of the samples. Following an ultrapure-water rinse of the residual soil, 3 mL AR solution was added,
95 and the material was shaken and again left to react at 20 °C for 15 hours. After centrifuging, the clear supernatant solution –
96 the ‘AR digest’ or ‘B’ sample – was removed and dried in the HEPA-filtered fume-hood. The lead isotope analyses discussed
97 in this study were performed on the AR digest, although additional AmAc results are also provided for a subset of samples,
98 but not discussed further.

99 Lead isotope analyses followed procedures described in Desem et al. (2022) and are briefly outlined below. Importantly, the
00 methodology allows for the analysis of samples without prior matrix removal, greatly improving sample throughput. Analyses
01 were performed using a Nu Instruments Attom SF-ICP-MS. Dried soil digests were redissolved in 2% HNO₃ run solutions
02 containing admixed high-purity thallium (1 ppb Tl), and diluted to provide ~1 ppb Pb in solution. Following the method of
03 Woodhead (2002), addition of natural, Pb-free Tl (with a nominal ²⁰⁵Tl/²⁰³Tl of 2.3871) allowed the correction of instrumental
04 mass bias effects during Pb-isotope analyses. Analyses of the National Institute of Standards & Technology (NIST) Common
05 Lead Isotopic Standard Reference Material SRM 981 (certificate of analysis available at
06 <https://tsapps.nist.gov/srmext/certificates/archives/981.pdf>; last access 4 February 2024) interspersed throughout the unknown
07 analyses were used to update the long term Pb vs Tl master correlations. Pb blanks for the combined leaching and chemical

08 procedures were typically <100 pg and are considered negligible relative to the amount of Pb being processed (typically
 09 hundreds of ng); as a result no blank corrections have been made. A small number of samples with low Pb concentrations
 10 exhibited very low signal sizes during analysis, resulting in correspondingly high analytical uncertainties. Samples producing
 11 within-run uncertainties of >1% relative (measured on the $^{207}\text{Pb}/^{204}\text{Pb}$ ratio) were discarded as being insufficiently precise to
 12 contribute meaningfully to the dataset.

13 2.3 Quality assessment

14 Although previous studies using the Attom SF-ICP-MS technique (e.g., Newman and Georg, 2012) used sample-standard-
 15 bracketing techniques to correct for instrumental mass bias during Pb-isotope analysis, in this study Tl doping was found to
 16 produce more precise, accurate and reproducible results. As the NIST SRM 981 Standard Reference Material was used to
 17 establish the Pb-Tl calibration (see above) SRM 981 values could not be used to assess analytical accuracy. Averages obtained
 18 for a variety of other, secondary reference materials measured during the course of this study, however, are consistent with
 19 accepted values (see Table 1), providing confidence in the analysis of unknowns.

20

21 **Table 1. Pb isotope data obtained for geological reference materials run concurrently with the analyses reported in this paper and**
 22 **employed as secondary standards. Nominal values are derived from GeoREM (Jochum et al., 2007).**

Standard	Value	$^{206}\text{Pb}/^{204}\text{Pb}$	$^{207}\text{Pb}/^{204}\text{Pb}$	$^{208}\text{Pb}/^{204}\text{Pb}$	$^{207}\text{Pb}/^{206}\text{Pb}$	$^{208}\text{Pb}/^{206}\text{Pb}$
BCR-2 (<i>n</i> = 39)	Nominal	18.754	15.622	38.726	0.8329	2.0649
	Average	18.74	15.61	38.71	0.8328	2.0665
	%2SD	0.43	0.47	0.42	0.23	0.32
	%deviation	-0.08	-0.09	-0.04	-0.01	0.08
BR (<i>n</i> = 11)	Nominal	19.215	15.606	39.135	0.8122	2.0367
	Average	19.23	15.69	39.16	0.8164	2.0372
	%2SD	0.50	0.62	0.88	0.26	0.26
	%deviation	0.07	0.54	0.06	0.52	0.02
AGV-2 (<i>n</i> = 13)	Nominal	18.870	15.616	38.554	0.8275	2.0431
	Average	18.90	15.64	38.60	0.8279	2.0420
	%2SD	0.27	0.35	0.40	0.27	0.17
	%deviation	0.15	0.17	0.11	0.05	-0.05
JB-2 (<i>n</i> = 9)	Nominal	18.342	15.561	38.274	0.8484	2.0867
	Average	18.42	15.65	38.46	0.8493	2.0871
	%2SD	0.68	0.60	0.71	0.29	0.34
	%deviation	0.40	0.60	0.48	0.11	0.02

23

24 We see very good agreement between our SF-ICP-MS data and nominal accepted values for the well-known and described
 25 reference materials BCR-2 and AGV-2 (both produced by the United States Geological Survey). Agreement was slightly

26 poorer for the two other reference materials utilised — BR (produced by the Centre de Recherches Pétrographiques et
27 Géochimiques – CRPG - Nancy) and JB-2 (produced by the Japanese Geological Survey) — especially for ^{207}Pb -based ratios
28 but these have been relatively little studied and at least some of this variation may therefore be the result of uncertainty in
29 assigned literature values. Based upon the data for the BCR-2 and AGV-2 reference materials, for which we have the most
30 analyses and for which accepted values are more robust, our accuracy is estimated to be typically $<0.17\%$. More detailed
31 assessments of data quality, including comparisons with other instrumental techniques for Pb-isotope analysis, can be found
32 in Desem et al. (2022) and are not re-iterated here.

33

34

35 One hundred and six field duplicate sample pairs (NGSA field duplicates, collected at a median distance of ~ 100 m from one
36 another on the same landscape unit, see Cooper et al., 2010) were analysed using the TOS <2 mm sample, and returned a
37 median relative standard deviations for ratios $^{206}\text{Pb}/^{204}\text{Pb}$, $^{207}\text{Pb}/^{204}\text{Pb}$, $^{208}\text{Pb}/^{204}\text{Pb}$, $^{207}\text{Pb}/^{206}\text{Pb}$, and $^{208}\text{Pb}/^{206}\text{Pb}$ of 0.50%, 0.24%,
38 0.43%, 0.30%, and 0.34%, respectively. The relative standard deviations from field duplicates includes natural variability
39 (mineralogical/chemical heterogeneity of the alluvial deposit), as well as sample collection, preparation, and analysis
40 uncertainties. Overall, we consider that the quality of the data presented herein is adequate for the purpose of constructing
41 isoscapes at the regional scale.

42 **2.4 Data presentation**

43 Data management and analysis, including visualisation, were performed using Microsoft Excel (v.2306), IMDEX ioGas
44 (v.8.0), and open software QGis (v.3.16).

45 **3 Results and discussion**

46 **3.1 Statistics**

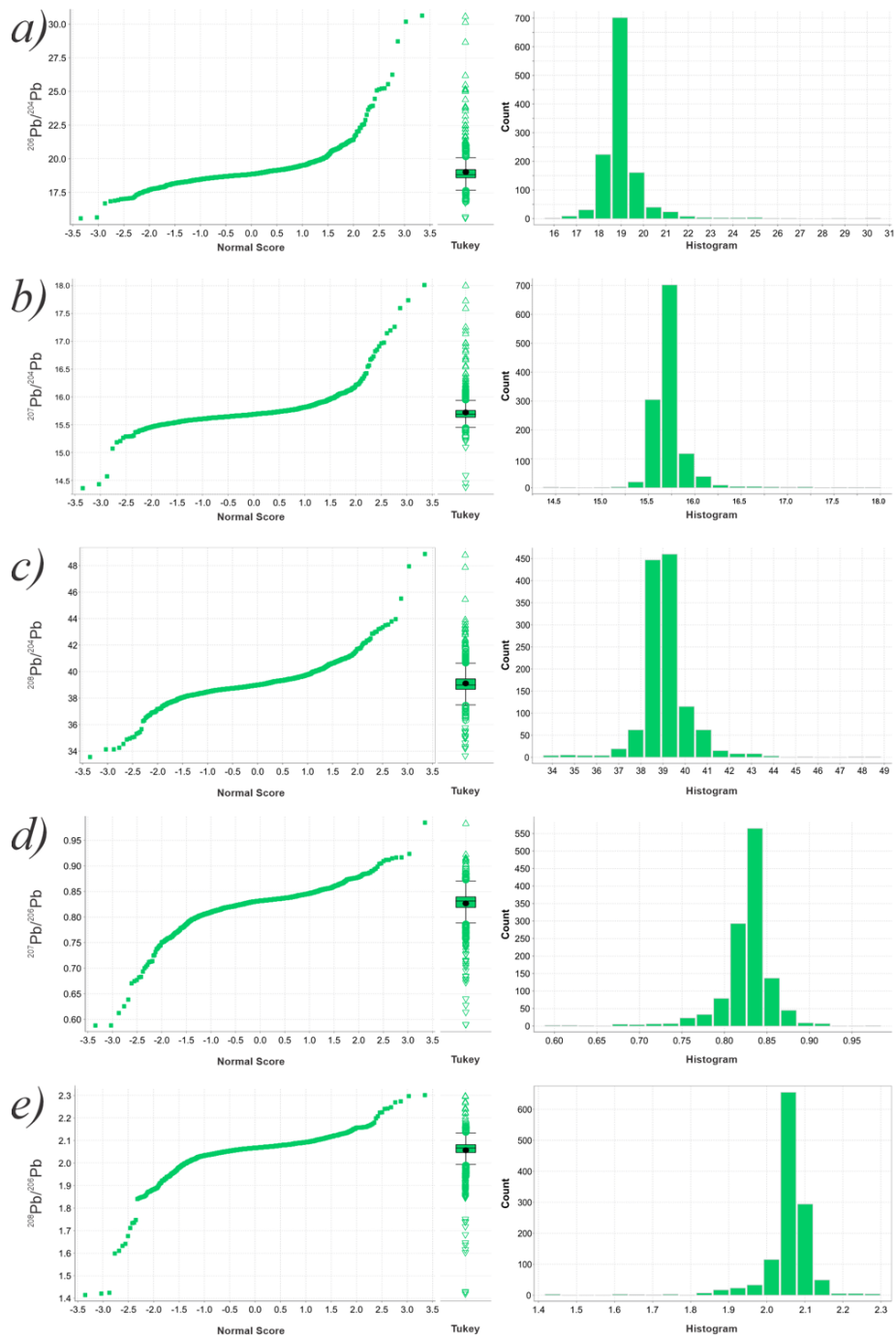
47 The overall results obtained in this study are summarised in Table 2. Normal score, Tukey boxplot and histogram distributions
48 of the $^{206}\text{Pb}/^{204}\text{Pb}$, $^{207}\text{Pb}/^{204}\text{Pb}$, $^{208}\text{Pb}/^{204}\text{Pb}$, $^{207}\text{Pb}/^{206}\text{Pb}$, and $^{208}\text{Pb}/^{206}\text{Pb}$ ratios are shown in Figure 2. It can be seen that these
49 distributions are fairly ‘normal’ (Gaussian, or ‘balanced’ about the median), ‘tight’ (small interquartile ranges, or ‘boxes’, and
50 widespread lower and upper quartiles), and with variable kurtosis and skewness.

51

52 Table 2. Summary statistics of the Pb isotope data obtained from 1207 National Geochemical Survey of Australia (NGSA) and 12
 53 Northern Australia Geochemical Survey (NAGS) TOS coarse analyses by Aqua Regia digestion following Ammonium Acetate leach
 54 (n = 1219). See text for further details.

Value	²⁰⁶ Pb/ ²⁰⁴ Pb	²⁰⁷ Pb/ ²⁰⁴ Pb	²⁰⁸ Pb/ ²⁰⁴ Pb	²⁰⁷ Pb/ ²⁰⁶ Pb	²⁰⁸ Pb/ ²⁰⁶ Pb
Minimum	15.56	14.36	33.56	0.5880	1.4149
Maximum	30.64	18.01	48.87	0.9847	2.3002
Range	15.08	3.65	15.32	0.3968	0.8854
Mean	19.05	15.72	39.12	0.8270	2.0568
Standard Deviation	1.07	0.22	1.09	0.03	0.07
Coefficient of Variation (%)	5.63	1.41	2.80	3.80	3.28
Median	18.84	15.69	38.99	0.8318	2.0665
Robust Standard Deviation	0.45	0.09	0.59	0.02	0.03
Robust Coefficient of Variation (%)	2.41	0.58	1.50	1.86	1.27
Kurtosis	33.17	30.12	13.26	12.95	27.41
Skewness	4.30	3.45	1.26	-2.22	-3.74

55



56

57 **Figure 2. Normal score, Tukey boxplot and histogram distributions for (a) $^{206}\text{Pb}/^{204}\text{Pb}$, (b) $^{207}\text{Pb}/^{204}\text{Pb}$, (c) $^{208}\text{Pb}/^{204}\text{Pb}$, (d) $^{207}\text{Pb}/^{206}\text{Pb}$,**
 58 **and (e) $^{208}\text{Pb}/^{206}\text{Pb}$ isotope ratios obtained for Australian TOS coarse samples by Aqua Regia digestion following Ammonium Acetate**
 59 **leach ($n = 1219$). Mean, outlier and far outlier values are shown on the Tukey boxplots as dots, circles, and triangles, respectively.**
 60 **See text for further details.**

61 3.2 Validation

62 3.2.1 Intra-catchment variation

63 One NGSa catchment was also sampled at higher resolution by several NAGS samples, providing an opportunity to test the
64 fundamental assumption underpinning the catchment-based sampling strategy of the NGSa, namely that one catchment outlet
65 sediment sample fairly represents an average value for the whole catchment. In this case NGSa sample 2007190096 is from
66 the Newcastle Creek catchment (TS0715), approximately 100 km northeast of Elliott in the NT, which was also sampled by
67 12 NAGS samples. The mean of these 12 NAGS samples is within 0.62 standard deviation of the singular catchment-outlet
68 NGSa value for $^{206}\text{Pb}/^{204}\text{Pb}$, $^{207}\text{Pb}/^{204}\text{Pb}$, $^{208}\text{Pb}/^{204}\text{Pb}$, and $^{207}\text{Pb}/^{206}\text{Pb}$; for the isotopic ratio $^{208}\text{Pb}/^{206}\text{Pb}$ it is within 1.11 standard
69 deviation (Table 3). All samples are TOS coarse fractions digested in AR after an AmAc leach as described above. The
70 comparison supports the premise of the NGSa sampling strategy, namely that catchment outlet sediments are geochemically
71 and mineralogically representative of their overall catchment, yet of course recognises that intra-catchment variation is
72 occurring and can be significant.

73

74 **Table 3. Pb isotope data obtained from 12 Northern Australia Geochemical Survey (NAGS) samples in catchment TS0715, compared**
75 **to the National Geochemical Survey of Australia (NGSA) catchment outlet sample for the same catchment. The Difference (Average**
76 **NAGS – NGSA) is shown as absolute values and normalised to the standard deviation (SD) of the NAGS values. See text for further**
77 **details.**

Samples in catchment TS0715	$^{206}\text{Pb}/^{204}\text{Pb}$	$^{207}\text{Pb}/^{204}\text{Pb}$	$^{208}\text{Pb}/^{204}\text{Pb}$	$^{207}\text{Pb}/^{206}\text{Pb}$	$^{208}\text{Pb}/^{206}\text{Pb}$
20173120170 (NAGS)	17.02	15.07	34.54	0.8853	2.0284
20173120227 (NAGS)	19.11	15.74	39.04	0.8239	2.0432
20173120413 (NAGS)	18.97	15.66	38.68	0.8249	2.0399
20173120558 (NAGS)	18.99	15.65	38.77	0.8242	2.0396
20173120577 (NAGS)	18.90	15.65	38.77	0.8284	2.0508
20173120699 (NAGS)	19.05	15.63	38.92	0.8209	2.0438
20173120722 (NAGS)	19.09	15.67	38.89	0.8206	2.0359
20173120774 (NAGS)	19.10	15.65	38.78	0.8196	2.0309
20173120957 (NAGS)	18.98	15.66	38.65	0.8246	2.0362
20173120982 (NAGS)	18.93	15.73	39.07	0.8306	2.0637
20173121029 (NAGS)	18.93	15.64	38.94	0.8261	2.0568
20173121195 (NAGS)	19.01	15.64	38.98	0.8233	2.0517
Average (NAGS)	18.84	15.62	38.50	0.8294	2.0434
SD (NAGS)	0.58	0.18	1.26	0.0179	0.0106
2007190096 (NGSA)	19.13	15.69	39.28	0.8210	2.0552
Difference	-0.29	-0.07	-0.78	0.0084	-0.0118
Difference / SD (NAGS)	-0.50	-0.43	-0.62	0.47	-1.11

78

79 **3.2.2 Regional scale isotopic variation**

80 The regolith Pb isotope data, at the continental scale, are clearly governed by major crustal boundaries. At the highest level
 81 this is reflected in the more radiogenic signatures (e.g., higher $^{206}\text{Pb}/^{204}\text{Pb}$ ratios) in older terranes (i.e., west and northern
 82 Australia), compared with less radiogenic signatures of younger terranes (Tasman and New England Fold belts), but is also
 83 visible in data averages calculated for each of the ‘crustal elements’ indicated in Figure.1 and Table 4. At this scale the
 84 $^{206}\text{Pb}/^{204}\text{Pb}$ and $^{208}\text{Pb}/^{204}\text{Pb}$ isotope signatures exhibit the greatest variation since most ^{235}U decayed early in Earth history and
 85 thus changes in $^{207}\text{Pb}/^{204}\text{Pb}$ are more subdued compared to variations in the $^{206}\text{Pb}/^{204}\text{Pb}$ and $^{208}\text{Pb}/^{204}\text{Pb}$ signatures.

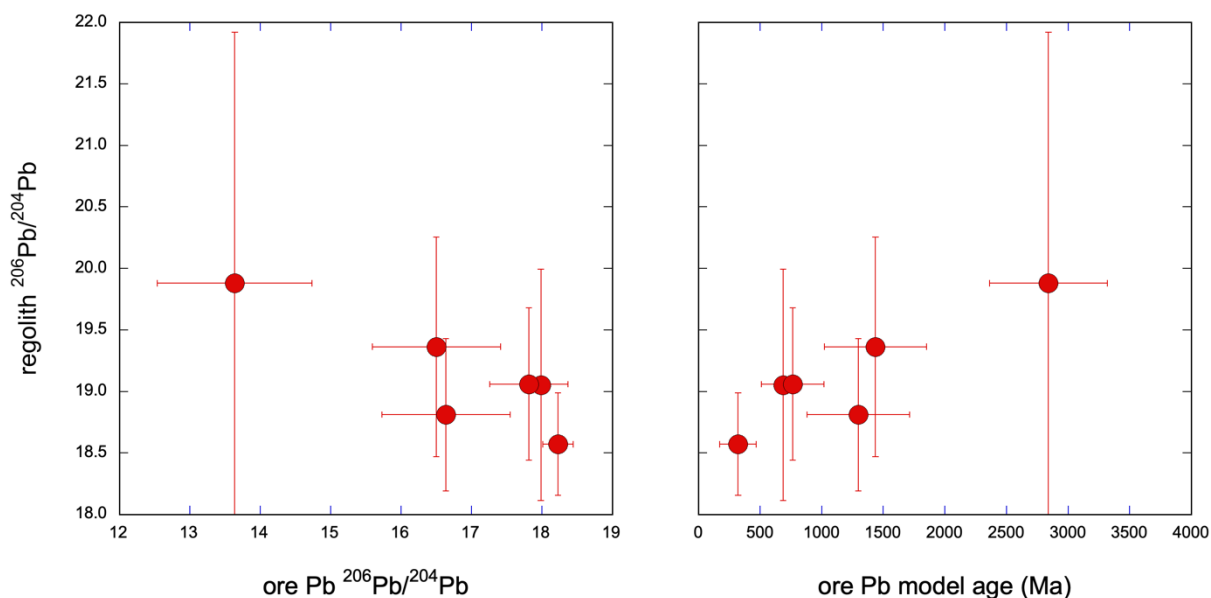
86 Regolith-derived data averages also broadly correlate with initial Pb signatures derived from a compilation of ore Pb data
 87 (Huston et al., 2019, 2021) and the terrane model ages derived from these data (Fig.3).

88

89 **Table 4. Regolith Pb isotope ratios from this study, averaged for each of the mega-crustal elements (Shaw et al., 1998), compared**
 90 **with ore Pb signatures and Stacey-Kramers model ages from Huston (2019, 2021).**

Mega-crustal element	$^{206}\text{Pb}/^{204}\text{Pb}$		$^{207}\text{Pb}/^{204}\text{Pb}$		$^{208}\text{Pb}/^{204}\text{Pb}$		Model age (Ma)
	This study	Huston et al. (2019)	This study	Huston et al. (2019)	This study	Huston et al. (2019)	
Pinjarra	19.05	17.985	15.79	15.710	39.50	38.677	688
West Australian	19.88	13.637	15.94	14.698	39.72	33.481	2840
South Australian	18.81	16.637	15.68	15.479	38.94	36.350	1298
Central Australian	19.06	17.814	15.75	15.684	39.56	38.129	765
North Australian	19.36	16.501	15.74	15.500	39.48	36.247	1436
Tasman	18.58	18.230	15.63	15.611	38.57	38.233	321

91



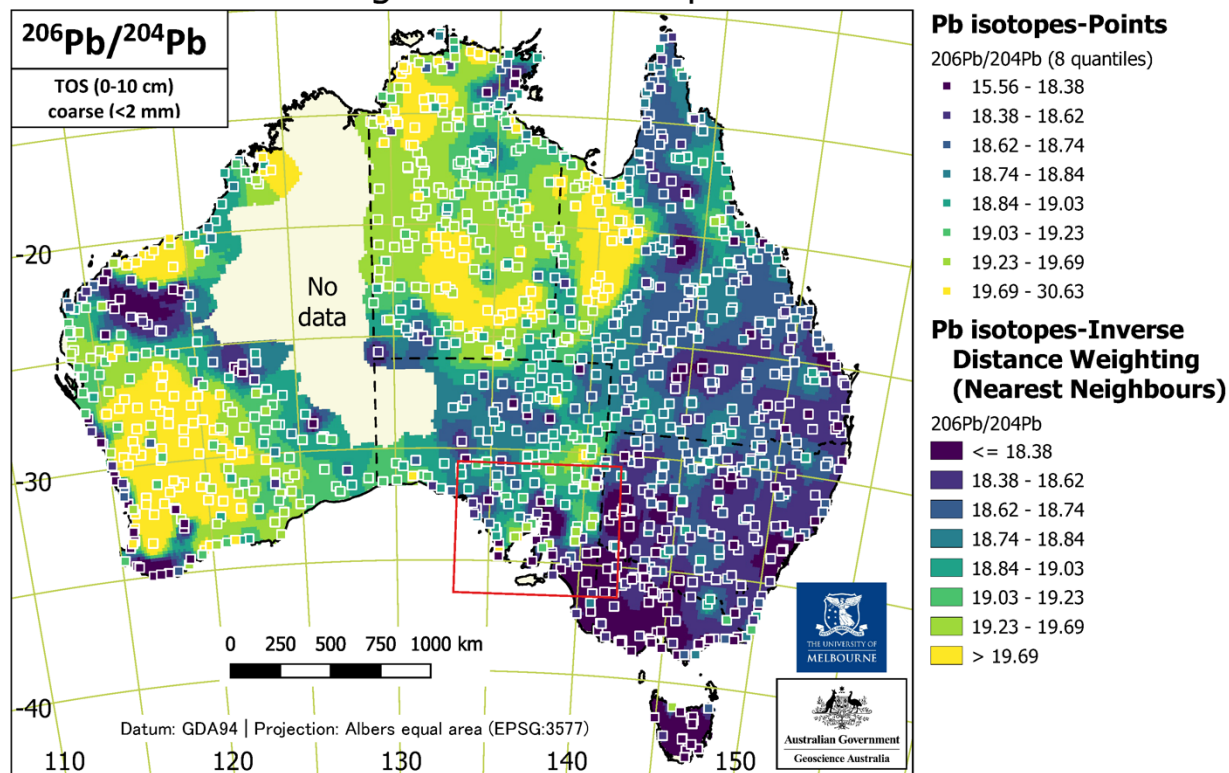
92

93 **Figure 3. Regolith vs ore Pb isotope averages for each mega-crustal element (left), and vs model ages (right) derived for these from**
 94 **ore Pb data (Huston et al., 2019, 2021).**

95 **3.3 Isoscapes**

96 The Pb isotope maps (isoscapes) for the ratios $^{206}\text{Pb}/^{204}\text{Pb}$, $^{207}\text{Pb}/^{204}\text{Pb}$, $^{208}\text{Pb}/^{204}\text{Pb}$, $^{207}\text{Pb}/^{206}\text{Pb}$, and $^{208}\text{Pb}/^{206}\text{Pb}$ are presented
 97 below (Figures 4 to 8). Each map includes a series of ‘Points’ coloured according to eight quantile classes for binning overlain
 98 on a raster surface coloured in the same way. The raster is an ‘Inverse distance weighting’ (IDW) interpolation produced with
 99 the **Grid (IDW with Nearest Neighbor Searching)** or **invdistnn** GDAL tool in QGIS. The ‘inverse distance to a power’
 00 gridding method is a weighted average interpolator. Sample points are weighted during interpolation such that the influence
 01 of one point relative to another declines with the distance from the unknown pixel to be estimated. Here, a weighting power
 02 of 2, minimum/maximum nearest neighbouring points of 6/12, and grid cells of $0.25^\circ \times 0.25^\circ$ resolution are the parameters
 03 used. The rectangular rasters thus produced were subsequently clipped to a custom polygon combining the Australian coastline
 04 with the area of ‘No data’ in the NGS coverage using the **Clip Raster by Mask Layer** or **gdalwarp –cutline** GDAL tool in
 05 QGIS.

Regolith Lead Isoscape of Australia



06

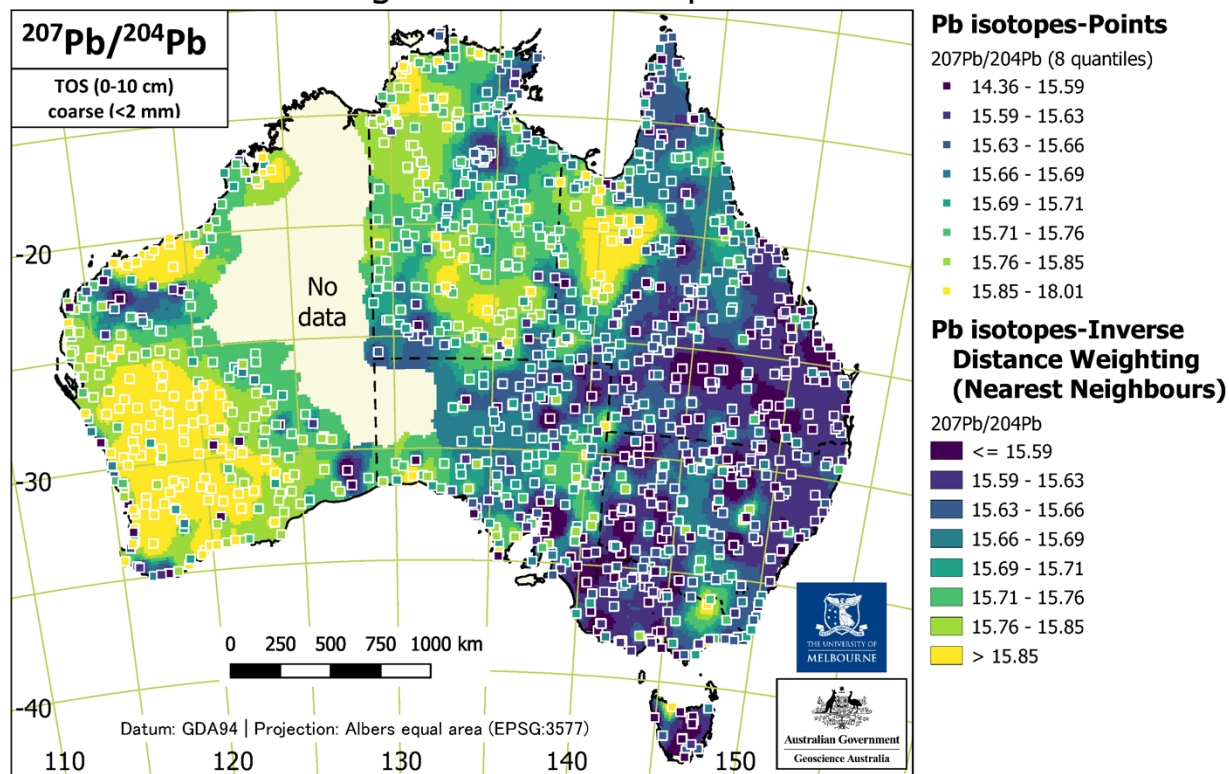
07

Figure 4. Regolith Pb isoscape of Australia for $^{206}\text{Pb}/^{204}\text{Pb}$ with data points (AR digestion of TOS coarse samples) classed by

08

quantiles and overlain on an IDW interpolation raster classed identically. The red rectangle indicates the location of Figure 9. See

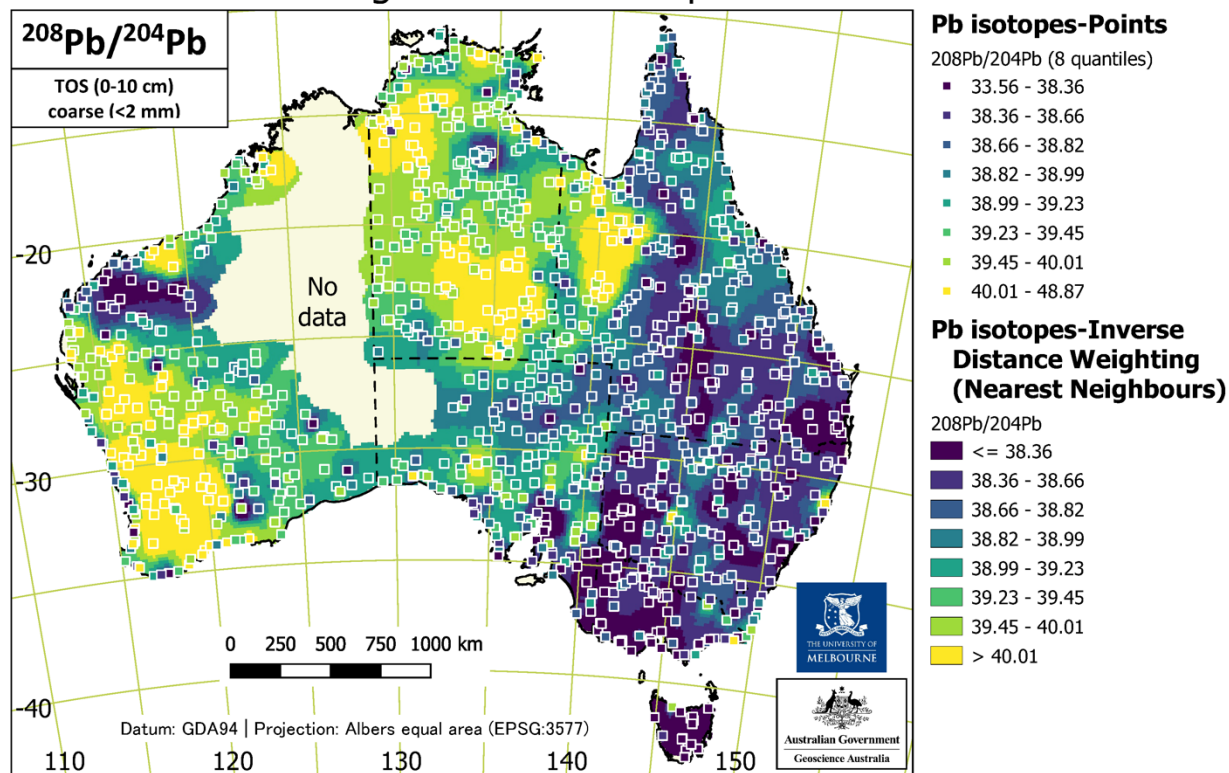
Regolith Lead Isoscape of Australia



10

11 **Figure 5. Regolith Pb isoscape of Australia for $^{207}\text{Pb}/^{204}\text{Pb}$ with data points (AR digestion of TOS coarse samples) classed by quantiles**
 12 **and overlain on an IDW interpolation raster classed identically. See text for further details.**

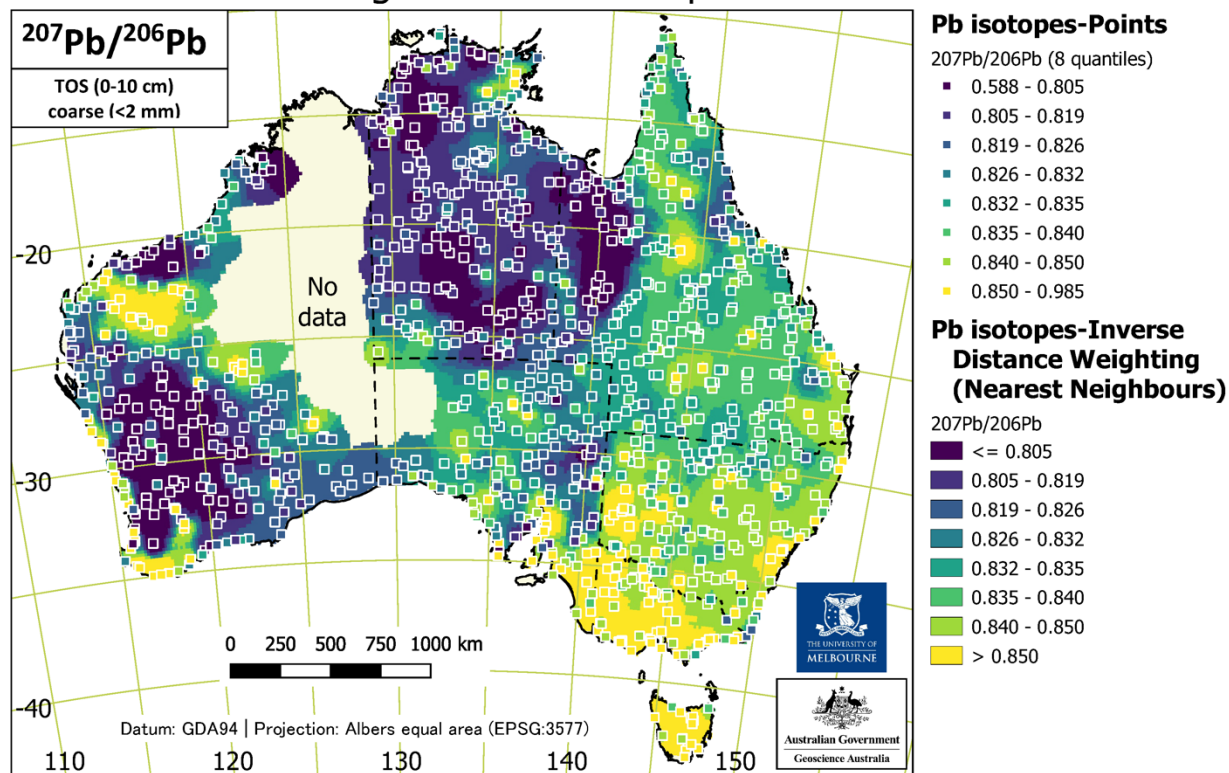
Regolith Lead Isoscape of Australia



13

14 **Figure 6. Regolith Pb isoscape of Australia for $^{208}\text{Pb}/^{204}\text{Pb}$ with data points (AR digestion of TOS coarse samples) classed by quantiles**
15 **and overlain on an IDW interpolation raster classed identically. See text for further details.**

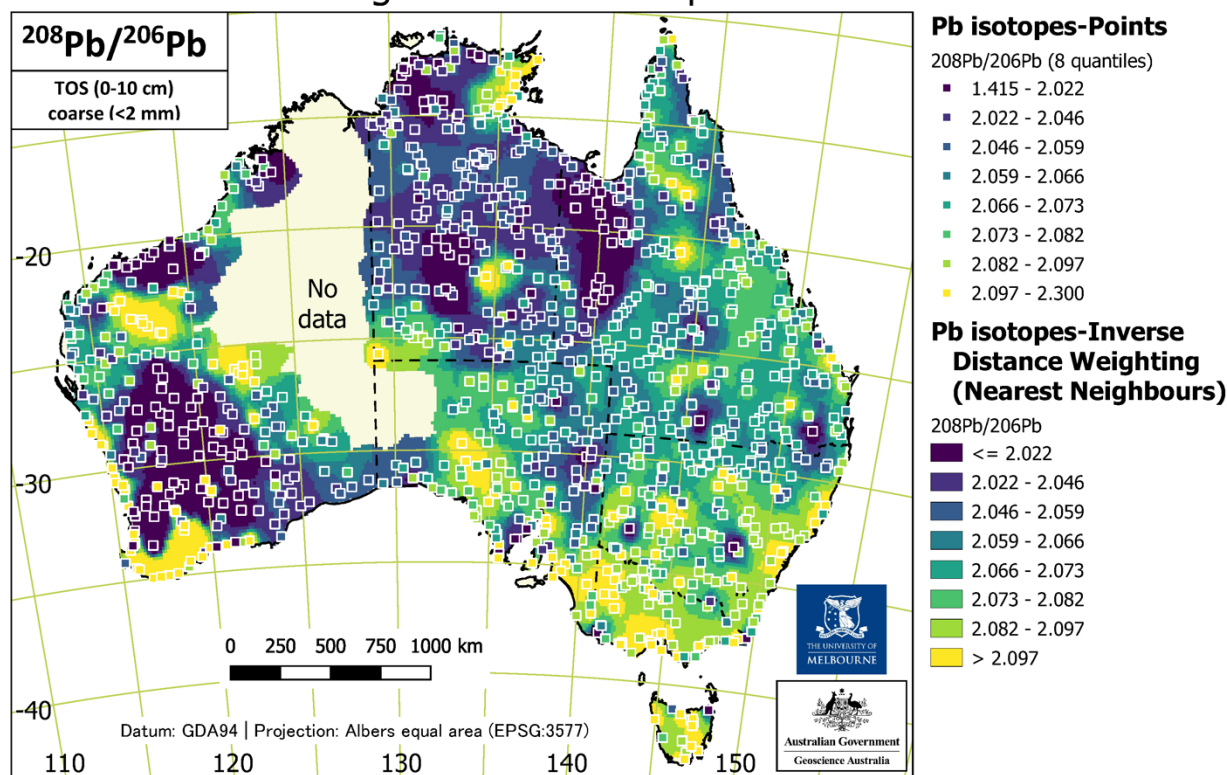
Regolith Lead Isoscape of Australia



16

17 **Figure 7. Regolith Pb isoscape of Australia for $^{207}\text{Pb}/^{206}\text{Pb}$ with data points (AR digestion of TOS coarse samples) classed by**
18 **quantiles and overlain on an IDW interpolation raster classed identically. See text for further details.**

Regolith Lead Isoscape of Australia



19

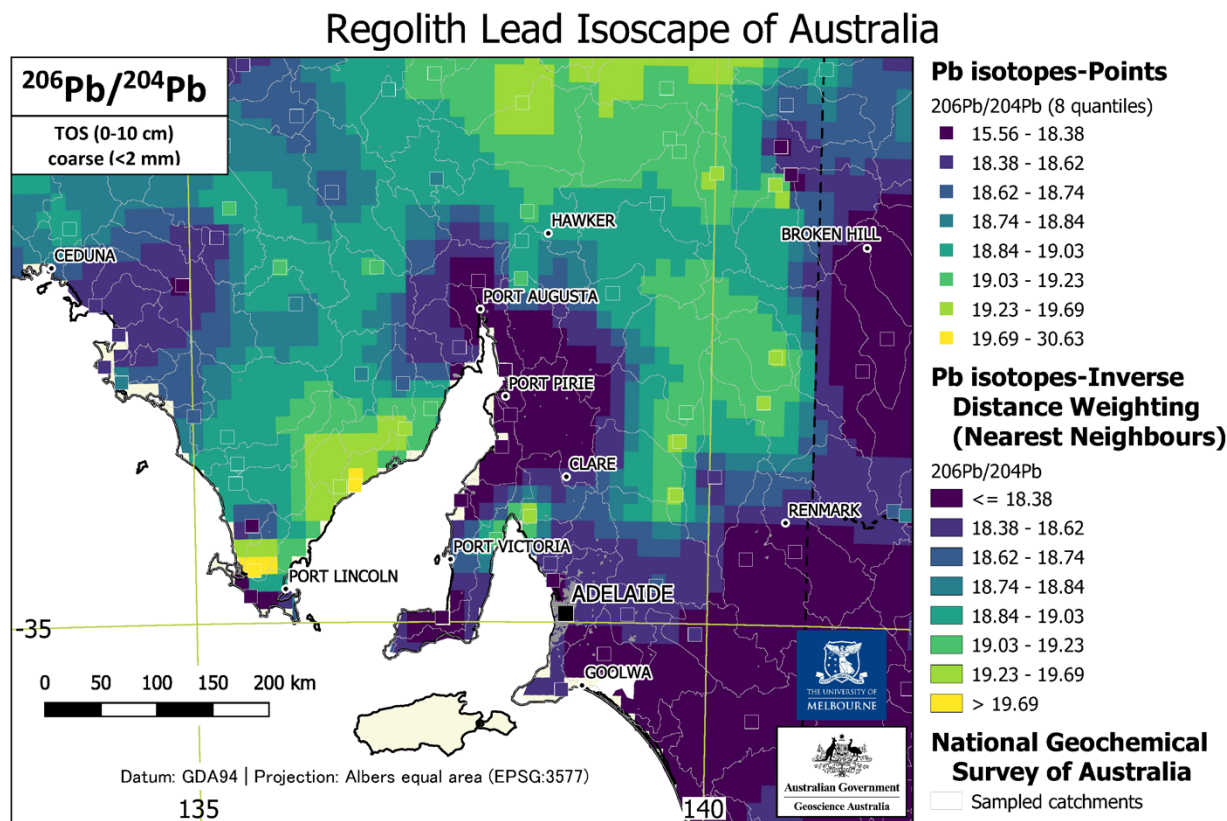
20 **Figure 8. Regolith Pb isoscape of Australia for $^{208}\text{Pb}/^{206}\text{Pb}$ with data points (AR digestion of TOS coarse samples) classed by quantiles**
21 **and overlain on an IDW interpolation raster classed identically. See text for further details.**

22 All isoscape IDW-NN geotiff rasters are downloadable as per the Data subsection.

23 3.4 Applications

24 The present Pb isoscapes can be applied to studies of the evolution of the Australian crust, regional mineral exploration, and
25 baselines for environmental investigations. The former two will be developed elsewhere, but the latter is illustrated below with
26 an example from data obtained close to the Port Pirie smelter in South Australia. Port Pirie is the locality of the largest Pb
27 smelter and refinery in the southern hemisphere; a Pb smelter has been active there over 130 years (SA EPA). The widespread
28 contamination of the area surrounding the smelter by means of windblown Pb dust is well documented in the literature (e.g.,
29 Gulson et al., 1981). Our TOS regolith data (Figure 9) show pronounced unradiogenic signatures (e.g., lower $^{206}\text{Pb}/^{204}\text{Pb}$ ratios)
30 adjacent to the area, which likely reflect a profound overprint from the ores processed in the facility, despite the application of
31 the AmAc pre-leach to these samples. During its >100 year history, the dominant source of the feedstock for the smelter was

32 from the geologically ancient (1600 million years: Gulson, 1984) Broken Hill deposit in New South Wales (Body et al., 1988)
 33 and, later, the Teutonic Bore mine in Western Australia. The low $^{206}\text{Pb}/^{204}\text{Pb}$ ratios in the smelter emissions are consistent with
 34 the low ratios of 16.00 in the Broken Hill ore (Gulson, 1984). For two NGS sites — 2007190995 located south of the Port
 35 Pirie Pb smelter and 2007190228 from north of Port Pirie location — we analysed both TOS and BOS sample aliquots, with
 36 the TOS coarse fraction producing less radiogenic Pb isotope signatures compared to the BOS fraction samples. This further
 37 suggests that most of the anthropogenic contamination resides in the surface layer (recent deposits). The bottom fraction
 38 samples for both locations are very similar to one another and likely reflect the signature of floodplain deposits formed prior
 39 to the initiation of smelting activities started and therefore provide a more reliable geogenic signature. The isotopic profiles in
 40 this study are consistent with those identified by Gulson et al. (1981).



41
 42 **Figure 9. Regional detail of the regolith Pb isoscape of Australia in the vicinity of the Pt Pirie smelter, South Australia, for $^{206}\text{Pb}/^{204}\text{Pb}$**
 43 **with data values (AR digestion of TOS coarse samples) classed by quantiles and overlain on an IDW interpolation raster classed**
 44 **identically. The NGS catchments are shown by the thin grey polygons. See text for further details.**

45 **4 Data availability**

46 The regolith Pb isotope dataset of Australia is publicly available (Desem et al., 2023;
47 <http://dx.doi.org/10.26186/5ea8f6fd3de64>).

48 **5 Conclusions**

49 New national-scale regolith lead (Pb) isoscapes for Australia are presented for the ratios $^{206}\text{Pb}/^{204}\text{Pb}$, $^{207}\text{Pb}/^{204}\text{Pb}$, $^{208}\text{Pb}/^{204}\text{Pb}$,
50 $^{207}\text{Pb}/^{206}\text{Pb}$, and $^{208}\text{Pb}/^{206}\text{Pb}$. The results of this study suggest that the isotopic signatures obtained from transported regolith in
51 Australia are dominated by Pb from the catchment bedrock geology. This influence is more easily visible in older (i.e. Archaean
52 and Proterozoic) terranes, simply because of the greater opportunity for radiogenic ingrowth here. This is demonstrated by the
53 correlation of Pb signatures with major crustal elements and their respective geological model ages. Exogenous
54 (anthropogenic) inputs of Pb have been detected at some sample locations and provide further encouragement for the utilisation
55 of the new Pb isoscapes in source attribution for environmental studies. An example from around the Port Pirie Pb smelter is
56 developed for illustration of this application. Other potential applications of this dataset include studies of the crustal evolution
57 of Australia, and using Pb isotopes for mineral exploration.

58 **Author contributions**

59 CD provided Investigation (Pb isotope analysis), Validation, and Writing – original draft.

60 PdC provided Data curation, Formal analysis, Resources (samples), Validation, Visualization, and Writing – original draft,
61 reviewing and editing.

62 JW provided Project administration, Methodology, Supervision, and Writing – original draft, reviewing and editing.

63 RM Supervision, Validation (standards data), Methodology

64 GC Supervision, Methodology

65 **Competing interests**

66 The contact author has declared that none of the authors has any competing interests.

67 **Disclaimer**

68 This paper is published with the permission of the Chief Executive Officer, Geoscience Australia.

69 **Acknowledgements**

70 The National Geochemical Survey of Australia (NGSA) project would not have been possible without Commonwealth funding
71 through the “Onshore Energy Security Program” (<http://www.ga.gov.au/ngsa>, last access: 5 September 2023), and Geoscience
72 Australia appropriation. The Northern Australia Geochemical Survey (NAGS) project was funded under the “Exploring for
73 the Future” programme (<https://eftf-production.ga.gov.au/northern-australia-geochemical-survey>, last access: 5 September
74 2023) and Geoscience Australia appropriation. Collaboration with the geoscience agencies of all states and the Northern
75 Territory is gratefully recognized. We acknowledge all land owners and custodians, whether private, corporate, and/or
76 traditional, for granting access to the field sites for the purposes of sampling. We are also grateful to Geoscience Australia
77 laboratory staff for assistance with preparing and analysing the samples. We thank Geoscience Australia reviewers, David
78 Huston and Kathryn Waltenberg; journal reviewers, Brian Gulson and one anonymous reviewer, and the editorial team for
79 their detailed and constructive critique of our work.

80 **Financial support**

81 Analytical work was conducted as part of Candan Desem’s PhD studies supported financially by University of Melbourne
82 Research Scholarship, Baragwanath Geology Research Scholarship and the Albert Shimmins Fund, in addition to a PhD
83 Student Research Grant from the International Association of GeoChemists (IAGC).

84 This research has also been supported by the Australian Government (Exploring for the Future,
85 <https://www.eftf.ga.gov.au/about>, last access: 5 September 2023). Geoscience Australia's Exploring for the Future programme
86 provides pre-competitive information to inform decision-making by government, community, and industry on the sustainable
87 development of Australia's mineral, energy, and groundwater resources. By gathering, analysing, and interpreting new and
88 existing pre-competitive geoscience data and knowledge, we are building a national picture of Australia's geology and resource
89 potential. This leads to a strong economy, resilient society, and sustainable environment for the benefit of all Australians. This
90 includes supporting Australia's transition to net-zero emissions; strong, sustainable resources and agriculture sectors; and
91 economic opportunities and social benefits for Australia's regional and remote communities. The Exploring for the Future
92 programme, which commenced in 2016, is an 8-year, AUD 225 million investment by the Australian Government.

93 **References**

94 Adams, S., Grün, R., McGahan, D., Zhao, J.-X., Feng, Y., Nguyen, A., Willmes, M., Quaresimin, M., Lobsey, B., Collard, M.,
95 and Westaway, M. C.: A strontium isoscape of north-east Australia for human provenance and repatriation, *Geoarchaeol.*, 34,
96 231–251, <https://doi.org/10.1002/gea.21728>, 2019.

97 Bataille, C. P., Crowley, B. E., Wooller, M. J., and Bowen, G. J.: Advances in global bioavailable strontium isoscapes,
98 *Palaeogeogr. Palaeoclimatol.*, 555, 109849, <https://doi.org/10.1016/j.palaeo.2020.109849>, 2020.

99 Bing-Quan, Z., Yu-Wei, C., and Xiang-Yang, C.: Application of Pb isotopic mapping to environment evaluation in China.
100 *Chem. Speciation Bioavail.*, 14, 49–56, <https://doi.org/10.3184/095422902782775335>, 2002.

101 Body, P.E., Inglis, G.R., Mulcahy, D.E.: Lead contamination in Port Pirie South Australia. SADEP Report number 101, SA
102 Department of Environment and Planning, Adelaide. 87p., 1988.

103 Bowen, G. J., West, J. B., Vaughn, B. H., Dawson, T. E., Ehleringer, J. R., Fogel, M. L., Hobson, K., Hoogewerff, J., Kendall,
104 C., Lai, C.-T., Miller, C. C., Noone, D., Schwartz, H., and Still, C. J.: Isoscapes to address large-scale earth science challenges,
105 *EOS Trans. Am. Geophys. Union*, 90, 109–116, <https://doi.org/10.1029/2009EO130001>, 2009.

106 Carr, G. R., Korsch, M. J., Denton, G. J., Gatehouse, S., Law, A., Gray, D. R., Andrew, A. S.: AMIRA P618, Isotopic
107 Discrimination of Partial Leach, Geochemical Anomalies in Covered Terrains, Final Report, CSIRO Division of Earth Science
108 and Resource Engineering, CSIRO Report, EP0410117, 2011.

109 Chesson, L. A., Tipple, B. J., Howa, J. D., Bowen, G. J., Barnette, J. E., Cerling, T. E., and Ehrlinger, J. R.: Stable isotopes in
110 forensics applications, in: *Treatise on Geochemistry, Second Edition*, edited by: Holland H. D. and Turekian K. K., 14, 285–
111 317, <http://dx.doi.org/10.1016/B978-0-08-095975-7.01224-9>, 2014.

112 Cooper, M., Caritat, P. de, Burton, G., Fidler, R., Green, G., House, E., Strickland, C., Tang, J., and Wygralak, A.: National
113 Geochemical Survey of Australia: Field Data, Record, 2010/18, *Geosci. Austral.*, Canberra,
114 <https://doi.org/10.11636/Record.2011.020>, 2010.

115 de Caritat, P. and Cooper, M.: A continental-scale geochemical atlas for resource exploration and environmental management:
116 the National Geochemical Survey of Australia, *Geochem. Explo. Env. Anal.*, 16, 3–13, <https://doi.org/10.1144/geochem2014-322>, 2016.

117

118 de Caritat, P. and Cooper, M.: National Geochemical Survey of Australia: The Geochemical Atlas of Australia, Record,
119 2011/20, *Geosci. Austral.*, Canberra, <http://pid.geoscience.gov.au/dataset/ga/71973>, 2011.

120 de Caritat, P., Cooper, M., Lech, M., McPherson, A., and Thun, C.: National Geochemical Survey of Australia: Sample
121 Preparation Manual, Record, 2009/08, *Geosci. Austral.*, Canberra, <http://pid.geoscience.gov.au/dataset/ga/68657>, 2009.

122 de Caritat, P., Cooper, M., Pappas, W., Thun, C., and Webber, E.: National Geochemical Survey of Australia: Analytical
123 Methods Manual, Record, 2010/15, *Geosci. Austral.*, Canberra, <http://pid.geoscience.gov.au/dataset/ga/70369>, 2010.

124 de Caritat, P., Dosseto, A., and Dux, F.: A strontium isoscape of inland southeastern Australia, *Earth Syst. Sci. Data*, 14, 4271–
125 4286, <https://doi.org/10.5194/essd-14-4271-2022>, 2022.

26 de Caritat, P., Dosseto, A., and Dux, F.: A strontium isoscape of northern Australia, *Earth Syst. Sci. Data*, 15, 1655–1673,
27 <https://doi.org/10.5194/essd-15-1655-2023>, 2023.

28 de Caritat, P.: The National Geochemical Survey of Australia: review and impact, *Geochem. Explo. Env. Anal.*, geochem2022-
29 032, <https://doi.org/10.1144/geochem2022-032>, 2022.

30 Desem, C. U., de Caritat, P., Woodhead, J. D., Maas, R., and Carr, G.: National Geochemical Survey of Australia: Lead
31 Isotopes Dataset, *Geosci. Austral.*, Canberra [data set], <http://dx.doi.org/10.26186/5ea8f6fd3de64>, 2023.

32 Desem, C. U., Maas, R., Woodhead, J., Carr, G., and Greig, A.: The utility of rapid throughput single-collector sector-field
33 ICP-MS for soil Pb isotope studies, *Appl. Geochem.*, 143, <https://doi.org/10.1016/j.apgeochem.2022.105361>, 2022.

34 Evans, J. A., Pashley, V., Mee, K., Wagner, D., Parker Pearson, M., Fremondeau, D., Albarella, U., and Madgewick, R.:
35 Applying lead (Pb) isotopes to explore mobility in humans and animals. *PLoS ONE*, 17(10), e0274831,
36 <https://doi.org/10.1371/journal.pone.0274831>, 2022.

37 Gale, N. H. and Stos-Gale, Z. A.: Lead isotope analyses applied to provenance studies, in: *Modern Analytical Methods in Art
38 and Archaeology*, edited by: Ciliberto, E. and Spoto, G., Wiley, New York, ISBN: 978-0-471-29361-3, 503–584, 2000.

39 Gulson, B.L.: Uranium-lead and lead-lead investigations of minerals from the Broken Hill lodes and mine
40 sequence rocks. *Econ. Geol.* 79, 476-490, 1984.

41 Gulson, B.: Stable lead isotopes in environmental health with emphasis on human investigations. *Sci. Total Environ.*, 400, 75–
42 92, <https://doi.org/10.1016/j.scitotenv.2008.06.059>, 2008.

43 Gulson, B.L., Gillings, B.R., and Jameson, C.W.: Stable lead isotopes in teeth as indicators of past domicile
44 - a potential new tool in forensic science, *J. Forensic Sciences*, 42, 787-791, 1997.

45 Gulson, B.L., Mizon, K.J., Korsch, M.J., Palmer, J.M., and Donnelly, J.B.: Mobilisation of lead from human
46 bone tissue during pregnancy and lactation – a summary of long-term research, *Science Total Environ.*, 303, 79-
47 104, 2003.

48 Gulson, B. L., Tiller, K. G., Mizon, K. J., and Merry, R. H.: Use of lead isotopes to identify the source of lead contamination
49 near Adelaide, South Australia, *Env. Sci. Technol.*, 15, 691–696, <https://doi.org/10.1021/es00088a008>, 1981.

50 Hobson, K. A., Barnett-Johnson, R., and Cerling, T.: Using isoscapes to track animal migration, in: *Isoscapes*, edited by: West,
51 J. B., Bowen, G. J., Dawson, T. E., and Tu, K. P., Springer, Dordrecht, The Netherlands, 273–298, [https://doi.org/10.1007/978-
52 90-481-3354-3_13](https://doi.org/10.1007/978-90-481-3354-3_13), 2010.

53 Hsu, Y.-K. and Sabatini, B. J.: A geochemical characterization of lead ores in China: an isotope database for provenancing
54 archaeological materials. *Plos One*, 14, e0215973, <https://doi.org/10.1371/journal.pone.0215973>, 2019.

55 Huston, D. L., Champion, D. C., Ware, B., Carr, G., Maas, R., and Tessalina, S.: Preliminary National-Scale Lead Isotope
56 Maps of Australia, Record, 2019/001, *Geosci. Austral.*, Canberra, <http://dx.doi.org/10.11636/Record.2019.001>, 2019.

57 Huston, D. L., Doublier, M.P., Downes P.M.: Geological setting, age and endowment of major Australian mineral deposits –
58 a compilation. Record 2021/20, *Geosci Austral.*, Canberra, <http://dx.doi.org/10.11636/Record.2021.020>, 2021.

59 Jochum, K.P., Nohl, U., Herwig, K., Lammel, E., Stoll, B. and Hofman, A.W.: GeoREM: a new geochemical database for
60 Reference Materials and Isotopic standards. *Geostandards and Geoanalytical Research* 29 (3), 333-338,
61 <https://doi.org/10.1111/j.1751-908X.2005.tb00904.x>, 2005.

62 Lech, M. E., de Caritat, P., and McPherson, A. A.: National Geochemical Survey of Australia: Field Manual, Record, 2007/08,
63 *Geosci. Austral.*, Canberra, <http://pid.geoscience.gov.au/dataset/ga/65234>, 2007.

64 Main, P. T., Bastrakov, E. N., Wygralak, A. S., and Khan, M.: Northern Australia Geochemical Survey: Data Release 2 – Total
65 (Coarse Fraction), Aqua Regia (Coarse and Fine Fraction), and Fire Assay (Coarse and Fine Fraction) Element Contents,
66 Record, 2019/002, *Geosci. Austral.*, Canberra, <http://dx.doi.org/10.11636/Record.2019.002>, 2019.

67 Newman, K. and Georg, R.B.: The measurement of Pb isotope ratios in sub-ng quantities by fast scanning single collector
68 sector field-ICP-MS. *Chem. Geol.*, 304–305, 151–157, <https://doi.org/10.1016/j.chemgeo.2012.02.010>, 2012.

69 Reimann, C., Flem, B., Fabian, K., Birke, M., Ladenberger, A., Negrel, P., Demetriades, A., Hoogewerff, J., and GEMAS
70 Project Team: Lead and lead isotopes in agricultural soils of Europe – the continental perspective. *Appl. Geochem.*, 27, 532–
71 542, <https://doi.org/10.1016/j.apgeochem.2011.12.012>, 2012.

72 Scaffidi, B. K. and Knudson, K.J.: An archaeological strontium isoscape for the prehistoric Andes: understanding population
73 mobility through a geostatistical meta-analysis of archaeological $^{87}\text{Sr}/^{86}\text{Sr}$ values from humans, animals, and artifacts. *J.*
74 *Archaeol. Sci.*, 117, 10521, <https://doi.org/10.1016/j.jas.2020.105121>, 2020.

75 Shaw, R. D., Wellman, P., Gunn, P. J., Whitaker, A. J., and Tarlowski, C.Z.: Australian Crustal Elements (National Geoscience
76 Dataset), *Geosci. Austral.*, Canberra [data set], <http://pid.geoscience.gov.au/dataset/ga/21195>, 1998.

77 Weisler, M. and Woodhead, J.D.: Basalt Pb isotope analysis and the prehistoric settlement of Polynesia, *Proc. Nat. Acad. Sci.*,
78 92, 1881–1885, <https://doi.org/10.1073/pnas.92.6.1881>, 1995.

79 Willmes, M., Bataille, C. P., James, H. F., Moffat, I., McMorro, L., Kinsley, L., Armstrong, R. A., Eggins, S., and Grün, R.:
80 Mapping of bioavailable strontium isotope ratios in France for archaeological provenance studies, *Appl. Geochem.*, 90, 75–
81 86, <https://doi.org/10.1016/j.apgeochem.2017.12.025>, 2018.

- 82 Woodhead, J.D.: A simple method for obtaining highly accurate Pb isotope data by MC-ICP-MS, *Journal of Analytical Atomic*
83 *Spectrometry.*, 17, 1381-1385, <https://doi.org/10.1039/B205045E>, 2002.
- 84 Zuluaga, M. C., Norini, G., Ayuso, R., Nieto, J. M., Lima, A., Albanese, S., and De Vivo, B.: Geochemical mapping,
85 environmental assessment and Pb isotopic signatures of geogenic and anthropogenic sources in three localities in SW Spain
86 with different land use and geology, *J. Geoch. Explo.*, 181, 172–190, <https://doi.org/10.1016/j.gexplo.2017.07.011>, 2017.